Available online at www.sciencedirect.com
SCIENCE DIRECT
Polymer 46 (2005) 4533–4543
polymer
www.elsevier.com/locate/polymer

Understanding the structure development in hyperbranched polymers prepared by oligomeric A_2+B_3 approach: comparison of experimental results and simulations

S. Unal[a], C. Oguz[b], E. Yilgor[c], M. Gallivan[b], T.E. Long[a], I. Yilgor[c,*]

[a]*Department of Chemistry, Virginia Polytechnic Institute and State University, Blacksburg, VA 24061, USA*
[b]*School of Chemical and Biomolecular Engineering, Georgia Institute of Technology, Atlanta, GA 30332, USA*
[c]*Department of Chemistry, Koc University, Sariyer, 34450 Istanbul, Turkey*

Received 27 January 2005; received in revised form 23 March 2005; accepted 31 March 2005
Available online 22 April 2005

Abstract

Structure development in highly branched segmented polyurethaneureas based on oligomeric A_2+B_3 approach was investigated by experimental studies and kinetic Monte-Carlo simulations. In both simulations and experiments, hyperbranched polymers were produced by the slow addition of A_2 onto B_3. Experimental studies showed strong influence of solution concentration on the gel point and the extent of cyclization in the polymers formed. In polymerizations conducted at a solution concentration of 25% by weight gelation took place at the stoichiometric ratio $[A_2]/[B_3]=0.886$. This is somewhat higher than the theoretical ratio of 0.75. In very dilute solutions, such as 5% solids by weight, no gelation was observed although the stoichiometric amount of A_2 added well exceeded the theoretical amount for gelation. Both experimental studies by size exclusion chromatography (SEC) and kinetic Monte-Carlo simulations demonstrated a gradual increase in polymer molecular weights as more A_2 is added onto B_3. This was followed by a sharp increase in the polymer molecular weight as the gel point is approached. A very similar behavior was observed for the polydispersity values of the polymers formed. Kinetic Monte-Carlo simulations performed at different cyclization ratios showed very good agreement with experimental results.

Keywords: Hyperbranched polymers; Polyurethanes; Simulations

1. Introduction

Highly branched polymers, which include dendritic, hyperbranched or multibranched polymers, are interesting and versatile materials and display several unique properties when compared with their linear analogs. These include low solution and melt viscosities, high solubilities and the presence of very large number of functional end groups that offers the possibility for further modification for various specialty applications. On the other hand several important drawbacks of these hyperbranched materials, with the exclusion of dendrimers, are broad molecular weight distributions, irregular arm growth (branching) and a statistical distribution of functional end groups throughout the macromolecule formed. Hyperbranched polymers are also reported to display poor mechanical properties due to absence of entanglements.

A number of excellent reviews, which describe the synthetic methodologies for the preparation of a wide variety of hyperbranched and dendritic polymeric systems through condensation, addition or ring-opening reactions, are available [1–6]. These include polyesters [7–10], polyamides [11–13], poly(ester-amides) [14], polyphenylenes [15,16], poly(ether sulfones) [17–19], poly(etherketones) [20,21], polyethers [22,23], polyurethanes [24–29], polyureas [29,30], polycarbonates [31] and others [1–6]. In addition to the numerous reports on the synthesis and structural characterization of these materials, there are several recent articles on the theoretical treatment of these systems that describe the evolution of molecular weight, molecular weight distribution and the degree of branching in these polymers [32–36]. All of these studies follow the

* Corresponding author. Tel.: +90 212 338 1418; fax: +90 212 338 1559.
E-mail address: iyilgor@ku.edu.tr (I. Yilgor).

0032-3861/$ - see front matter © 2005 Elsevier Ltd. All rights reserved.
doi:10.1016/j.polymer.2005.03.073

pioneering theoretical work of Flory [37], where he statistically described the random polycondensation of AB_x type monomers to yield highly branched polymers.

Linear, segmented polyurethanes or thermoplastic polyurethanes (TPU), which consist of alternating hard and soft segments on the same macromolecular chain, are one of the most interesting and versatile classes of polymeric materials [38–40]. As a result, TPUs find wide range of applications in many diverse fields [41]. Superior mechanical and thermal properties of TPUs have been attributed to their micro-phase separated morphologies and strong hydrogen bonding between the hard segment domains [42–44]. Although linear and crosslinked polyurethanes have been known for over 50 years, first reports on the successful preparation of hyperbranched (dendritic) polyurethanes have appeared in 1993. Spindler and Frechet [24] used AB_2 type monomers which contained a hydroxyl (A) and two blocked isocyanate groups (B_2). Polymerization was conducted in refluxing THF under the catalytic action of dibutyltin dilaurate to produce a high molecular weight product which is end capped with an aliphatic alcohol. Kumar and Ramakrishnan [25] also used an AB_2 type monomer and reported the preparation of wholly aromatic hyperbranched polyurethane from 3,5-dihydroxybenzoylazides, using Curtius type rearrangement reactions. Later, Kumar and Ramakrishnan also reported one-pot synthesis of hyperbranched polyurethanes containing very short ethylene oxide spacer segments [26]. The starting material was 3,5-bis(ω-hydroxy oligoethyleneoxy)benzoyl azide, again an AB_2 type monomer. Ether spacer segments on these monomers consisted of fairly short di- and tri(ethylene oxide) units. Similarly Hong et al., [45] have also reported the preparation of hyperbranched polyurethanes starting with AB_2 type monomers that contained very short ethylene oxide units. Several other reports on the preparation of hyperbranched polyurethanes using AB_2 type monomers [46–48] and others [28,49,50] are also available. More recently Bruchmann and Schrepp [27] described a different, one-step approach for the preparation of hyperbranched polyurethaneureas, where they used commercially available AA* and B*B_2 type monomers. AA* monomer was a diisocyanate (isophorone diisocyanate or toluene diisocyanate) and B*B_2 monomer was an aminoalkanediol. Gao and Yan also proposed an A_2+CB_n route for hyperbranched polyurethanes [29].

We have been investigating the preparation and structure–property behavior of linear segmented polyurethanes and polyureas with different soft segments for over two decades. Recently, we demonstrated the preparation of segmented, hyperbranched polyurethaneureas using an oligomeric A_2+B_3 approach, where A_2 was an isocyanate end-capped polyether glycol, such as poly(tetramethylene oxide)glycol (PTMO) and B_3 was an aliphatic triamine [51,52]. These novel copolymers displayed mechanical properties comparable to their linear analogs. Due to very high reactivity of isocyanates and aliphatic amines, polymerization reactions were conducted at room temperature with the drop-wise addition of an A_2 solution into a B_3 solution with strong agitation. Conventional procedures in step-growth polymerization are to mix all the reactants together at the beginning of the polymerization reaction. In some cases, when the system is chain extended, a two-step procedure is used. The drop-wise addition of A_2 into B_3 offers advantages over the conventional method, which may include better control of the structural regularity or the architecture of the polymeric product.

In order to better understand the polymer structure development, degree of branching, average molecular weights and the molecular weight distributions of the hyperbranched copolymers herein, a combination of theoretical calculations and experimental studies were performed. Computational methods were based on Monte-Carlo simulations. Experimental studies included the monitoring of the growth in the molecular weight and polydispersity as a function of oligomeric A_2 addition and influence of solution concentration on the gel point.

2. Experimental

2.1. Materials

Bis(4-isocyanatocyclohexyl)methane (HMDI) (Bayer) and cyclohexyl isocyanate (CHI) (Aldrich) with purities of greater than 99.5% were used. Poly(tetramethylene oxide)-glycol (PTMO) (Du Pont) with number average molecular weight (M_n) of 2000 g/mol, polyoxyalkylenetriamine (Jeffamine T-403, Huntsman) (TRI) (Fig. 1), HPLC grade isopropyl alcohol (IPA), and tetrahydrofuran (THF) (Aldrich) were all used as received.

2.2. Experimental procedures

All reactions were conducted in 3-neck, round-bottom Pyrex flasks equipped with an overhead stirrer, addition funnel and nitrogen inlet. Isocyanate end-capped PTMO (A_2) (Fig. 1) was prepared in bulk at 80 °C under the catalytic action of 100 ppm of dibutyltin dilaurate (T-12). Polymerization reactions for the preparation of hyperbranched polymers based on PTMO were carried out in THF/IPA (25/75; v/v) solutions, at room temperature, under strong agitation. During the reactions oligomeric A_2 solution was always added into B_3 (TRI) solution drop-wise. In order to monitor the growth in the molecular weight of the products, samples were withdrawn from the reactor at different amounts of A_2 addition and end capped with CHI prior to analysis by size exclusion chromatography (SEC). In experiments where the influence of solution concentration on gelation and cyclization was investigated, HMDI was used as (A_2) and TRI as (B_3). In these experiments IPA was used as the reaction solvent and reactions were conducted at room temperature under very strong agitation. Duration of the experiments was usually less than 30 min to

Bis(4-isocyanatocyclohexyl)methane (HMDI)

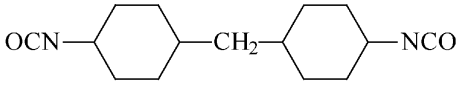

HMDI and capped PTMO-2000

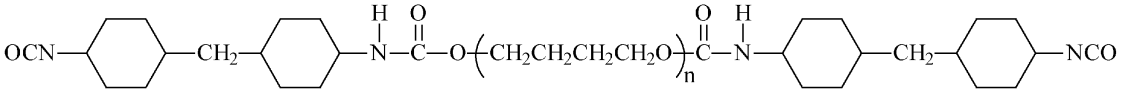

Polyoxyalkylenetriamine (TRI)

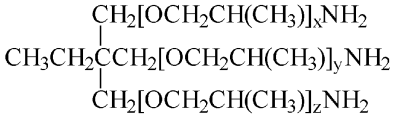

x+y+z=5.3 and <Mn> = 440 g/mol

Fig. 1. Chemical structures of monomeric and oligomeric A_2 and B_3.

ensure very small reaction between IPA and HMDI [53]. HMDI and TRI were separately dissolved in IPA at the specific concentration at which the reactions would be conducted. TRI solution was introduced into the reactor and the HMDI solution into the addition funnel. HMDI solution was added into the reactor drop-wise until the gelation is observed. Gel point was determined upon a sudden increase in the solution viscosity that was also confirmed by the formation of insoluble species in the reaction mixture. Stoichiometric amount of HMDI added at the gel point was determined for reactions carried out at different solution concentrations. These values are tabulated in Tables 1–3.

Table 1
Influence of the concentration of reaction medium on cyclization and gel point in hyperbranched polyureas formed by the slow addition of HMDI (A_2) onto TRI (B_3) in IPA at 23 °C

Solution concentration		A_2 added at gel point (%)	Estimated cyclization (%)
Weight (%)	Volume (%)		
25	19.7	88.6	13.6
20	15.5	94.3	19.3
20	15.5	93.3	18.3
15	11.5	97.0	22.0
15	11.5	97.4	22.4
10	7.5	107.6	32.6
10	7.5	107.5	32.5
7.5	5.6	120.5	45.6
5.0	3.7	>150 (no gel)	Very high

Dual reactions were performed to determine the reproducibility. Amount of cyclization was determined by subtracting the theoretical amount of A_2 needed at the gel point (75.0%) from the amount of A_2 used to reach the gel point experimentally.

2.3. Polymer characterization

IR spectra were obtained on a Nicolet NEXUS 670 FTIR spectrometer with a resolution of 2 cm^{-1}, using thin films cast on KBr disks. SEC measurements were conducted on a waters system that was equipped with three in-line PLgel 5 mm mixed-C columns, an autosampler, a 410 RI detector, a Viscotek 270 dual detector, and an in-line Wyatt

Table 2
Average molecular weights and molecular weight distributions of the polymers formed as a function of the amount of A_2 addition during the reaction of isocyanate terminated PTMO (A_2) and TRI (B_3)

Sample	A_2 addition (%)	$\langle M_n \rangle$ g/mol	$\langle M_w \rangle$ g/mol	M_w/M_n
PUU-25-1	50	11,700	17,600	1.50
PUU-25-2	60	16,670	26,200	1.57
PUU-25-3	71	24,900	54,800	2.20
PUU-25-4	76	24,700	141,000	5.71
PUU-25-5	84	43,400	255,000	5.88
PUU-25-6	89	Gel	Gel	–

Concentration of reaction medium is 25% solids by weight.

Table 3
Average molecular weights and molecular weight distributions of the polymers formed as a function of the amount of A_2 addition during the reaction of isocyanate terminated PTMO (A_2) and TRI (B_3)

Sample	A_2 addition (%)	$\langle M_n \rangle$ g/mol	$\langle M_w \rangle$ g/mol	M_w/M_n
PUU-10-1	69	16,200	23,900	1.48
PUU-10-2	81	16,600	37,000	2.23
PUU-10-3	95	26,300	74,700	2.84
PUU-10-4	102	25,200	116,000	4.60
PUU-10-5	110	63,000	392,000	6.22
PUU-10-6	112	Gel	Gel	–

Concentration of reaction medium is 10% solids by weight.

technologies miniDawn multiple angle laser light scattering (MALLS) detector. SEC measurements were performed at 40 °C in THF with a flow rate of 1 ml min^{-1} using polystyrene standards. Absolute molecular weights were obtained from MALLS detector.

2.4. Simulation algorithm

The development of structure during the polymerization reactions for hyperbranched polymers has been studied using different computational methods. The first approach includes development of kinetic models with kinetic differential equations and their numerical or analytical solution [54]. An alternative approach is using MC simulations [55]. Simulation of dendritic polymers in three dimensional space has also been employed [56]. While simulation of single dendritic structures is straightforward in three dimensional space, simulation of distributions is difficult because of the computational limitations imposed on the total number of units in the system [33]. A kinetic Monte-Carlo simulation technique, which is widely used to describe the structural evolution of molecules during polymerization reactions [55], was employed in the current study. Similar to the experimental procedure followed, initially, N molecules of B_3 are present in the system, and molecules of A_2 are then added sequentially during each simulation run.

The simulations consist of three steps. First, an A_2 monomer is added to the system. An unreacted B group is then selected, and is reacted with one of the two A groups. Each unreacted B group in the system has an equal probability of being selected, independent of molecular structure. In the third step, the remaining A group is reacted with another B group. When no cyclization is allowed, then the A group and the B group must be selected from different molecules, but each eligible B group has the same probability of selection.

Cyclization is a very important factor in step-growth reactions leading to the formation of dendritic and hyperbranched macromolecules [33,34,57–59]. In the simulation studies cyclization was taken into account in the following manner: an A group and a B group in the same molecule may react, but the selection probability for each B group is not equal. Instead, there is one selection probability for each B group in the same molecule as the A group, and a different probability for each B group not in that molecule. The selection probabilities are calculated from rates, using the kinetic Monte-Carlo (KMC) simulation algorithm of Bortz and co-workers [60], in which the selection probability of each event is proportional to its rate. In the simulations a variable cyclization parameter (γ) is defined, such that $\gamma = (k_c/k_{nc})/N$, in which k_c is the per end group rate of cyclization reaction, and k_{nc} is the rate when a non-cyclization reaction occurs. In the simulations rather than the individual values of k_c and k_{nc} their ratio is critical. During calculations the cyclization parameter (γ) was varied and the development of molecular characteristics such as M_n, M_w, polydispersity, degree of branching (DB), and cycles per molecule were determined. DB was calculated using: $DB = (D+T)/(D+L+T)$, where D, L and T indicate dendritic, linear and terminal units in the polymer. The dependence of cyclization probability on conversion is not explicitly built in KMC model used in simulations, because rate constants do not depend on conversion or molecular structure. However, as the monomer conversion increases, cyclization events become more likely due to the smaller number of molecules and the higher number of unreacted groups per molecule. Consequently, an increase in cyclization probability with conversion is implicitly built into the simulation model.

In the simulations presented here, $N = 1000$. Smaller and larger simulation sizes of $N = 100$, $N = 700$ and $N = 1300$ were also studied. The simulations with $N = 100$ differ significantly from the larger simulations, but the simulations with $N = 700$, $N = 1000$ and $N = 1300$ agree quantitatively, suggesting that the results reported in this study ($N = 1000$) are not dependent on the system size. The only exception occurs when there is no cyclization. In this case the simulations with $N = 700$ and $N = 1000$ differ near full conversion, mainly because the molecular weight is equal to the total weight in the system. However, this regime is not relevant to our experimental data and is not reported.

3. Results and discussion

It has been demonstrated that high strength, segmented, hyperbranched polyurethaneureas with tensile properties similar to their linear homologs can be prepared by the oligomeric $A_2 + B_3$ approach [52]. The polymerization procedure followed, where A_2 was added slowly onto B_3, is quite different than the conventional procedures employed for the preparation of step-growth polymers, which usually involves the addition of all reactants into the reactor at the beginning of the reaction. Slow addition of A_2 onto a large excess of B_3 is expected to provide a more controlled topology during polymer formation. It will also reduce the formation of side reactions and more importantly

the risk of gel formation during reactions, since the stoichiometric balance of the reactants will be controlled throughout the reaction.

Flory [37,61] has demonstrated that depending on the stoichiometry of the monomers and extent of reaction, step-growth polymerization reactions involving a mixture of difunctional (A_2) and trifunctional (B_3) monomers lead to the formation of hyperbranched or crosslinked polymers. According to Flory, for an A_2+B_3 system with all monomers initially present in the reaction mixture (the conventional procedure), assuming no side reactions (or no cyclization), the monomer conversions at gel point can be calculated by using the following equations [3,37,61]:

$$\alpha_c = \frac{1}{f-1} \tag{1}$$

$$\alpha_c = \frac{r p_A^2 \rho}{(1-r)p_A^2(1-\rho)} \tag{2}$$

where (α_c) is the probability of branching, (f) functionality of the branched units, (p_A and p_B) are the extent of reaction for A and B type monomers, (ρ) is the ratio of A groups on branch units to all A groups in the reaction mixture, and (r) is the ratio of the A groups to that of B groups. Flory showed that when $\alpha<\alpha_c$, gel formation is impossible, but may be possible when $\alpha>\alpha_c$ [37].

For an A_2+B_3 system, where equimolar amounts of A_2 and B_3 are initially present in the reaction mixture; $f=3$, $\alpha_c=1/2$ and $r=2/3$. Since all of our B groups are on branching units (B_3) $\rho=1$. Then Eq. (2) becomes:

$$\alpha_c = r p_A^2 = \frac{p_B^2}{r} \tag{3}$$

Substituting the values of $\alpha_c=1/2$ and $r=2/3$ in Eq. (3), $p_A=0.866$ and $p_B=0.577$ are calculated. This shows that in an A_2+B_3 system, where equimolar amounts of A_2 and B_3 are initially present in the reaction mixture, the gelation will take place when 57.7% of the B_3 monomer or 86.6% of the A_2 monomer has reacted. Alternatively, when the concentrations of A groups and B groups are equal ($r=1$), then theoretically, $p_A=p_B=0.707$ at the gel point.

In the idealized limit of slow A_2 addition into a large excess of B_3, each B group would be found in one of two possible states: (1) the B group is on an unreacted B_3 monomer, or (2) the B group has reacted with an A_2, which has also reacted with another B_3. Thus, the branching coefficient α is simply the conversion of B_3, referred to by Flory as p_B. For the limit of slow A_2 addition, we define the conversion of A_2 as $p_A=3/2p_B$, which is the molar percent of A_2 added into the reactor when compared with the number of moles of B_3 present in the reactor. Thus, at the critical point for gel formation, $p_B=0.50$ and $p_A=0.75$.

It is important to note that Flory's results apply only under the assumption that no cyclization has occurred, which is an unrealistic assumption at the gel point, as also noted by Flory. Furthermore, the condition $\alpha_c>1/2$ does not indicate that a gel has formed, but only that gel formation may be possible. In this study, Monte-Carlo simulations were used as an alternative to the theoretical results of Flory. This enables us to consider the effect of cyclization reactions, and to compare the molecular weight evolution in experiments and simulations as the gel point is approached, when A_2 is slowly added onto a large excess of B_3. We believe the computational and experimental approaches employed in this study will help to better understand the influence of reaction conditions on; (i) the development of the molecular structure and topology, such as degree of branching and extent of cyclization, (ii) polymer molecular weight, (iii) molecular weight distribution and (iv) the determination of the gel point during the preparation of hyperbranched polyurethaneurea copolymers through A_2+B_3 approach.

3.1. Influence of concentration of polymerization medium on gel point and extent of cyclization

As discussed above, in A_2+B_3 polymerizations that are conducted in bulk (no solvent effect) with all monomers added together into the reactor, theoretical gel point is at 86.6% conversion of A or 57.7% conversion of B groups [3,37]. However, as demonstrated by various groups [58,62–64], in kinetically controlled polycondensation reactions cyclization competes with linear polymer formation. When the polymerization is carried out in solution, there is even more tendency to form cyclic oligomers and/or macromolecules due to the well known cage effect [65]. Increase in the amount of cyclic species is also observed in thermodynamically controlled ring-chain equilibration reactions [66–68]. In order to understand the influence of the solvent concentration on gelation and cyclization during the preparation of highly branched polymers by oligomeric A_2+B_3 approach, we conducted experiments by varying the solution concentration between 5 and 25% solids. A major difference in our approach is the slow addition of A_2 onto B_3. As discussed above, in this case, the theoretical gel point is at 75% conversion of A or 50% conversion of B. In other reports [58,62–68] either AB_n type monomers were used or A_2 and B_3 were mixed together at the beginning of the polymerization reactions.

During our experiments A_2 (HMDI) and B_3 (TRI) solutions were prepared separately at specific concentrations (Table 1). B_3 solution is introduced into the reactor and A_2 solution into a graduated addition funnel. A_2 is added drop-wise onto B_3 solution under strong agitation. A_2 addition was continued until gelation. Amount of A_2 added at the gel point was determined at each concentration. The results are provided on Table 1, where the concentration of the reaction medium, amount of A_2 added and estimated level of cyclization are tabulated at each concentration. Experiments at 10, 15 and 20% solids were conducted twice to ensure the reproducibility of the experiments, which is

clearly demonstrated when the results are compared. The amount of A_2 added is the molar percent of A_2 added into the reactor when compared with the number of moles of B_3 present in the reactor. Under ideal conditions in slow A_2 addition on B_3, gelation is expected at 75% of A_2 addition. It is interesting to note that when the reaction is carried out at a fairly high solution concentration of 25% solids by weight, gelation takes place at 88.6% A_2 addition, which is higher than the amount expected by the theoretical calculations. When the concentration of the reaction medium is reduced to 20% solids by weight, gel point is reached at about 93.8% A_2 addition, which is again, much higher than the theoretical value. These results clearly indicate the extensive amount of intramolecular cyclization during polymerization reactions in solution. As the concentration of the reaction medium is further reduced to 15, 10 and 7.5% solids by weight, the amount of A_2 needed for gelation steadily increases to 97, 107.5 and 120.5%. When the reaction is carried out at a concentration of 5% solids by weight, gelation is never observed even though a very large stoichiometric excess of A_2 is added into the system! We believe this observation can only be explained by cyclization. In Table 1, an estimate of the extent of cyclization for reactions at different concentrations is provided in the last column. Cyclization was calculated by subtracting the theoretical amount of A_2 needed for gelation (75%) from the amount of A_2 needed to reach the gel point experimentally.

3.2. SEC studies on determination of polymer molecular weight as a function of A_2 addition

After determination of the experimental gel points in A_2+B_3 polymerization as a function of the solution concentration using low molecular weight A_2 (HMDI) and B_3 (TRI) monomers, we started investigating the development of polymer molecular weight and gel point as a function of oligomeric A_2 addition into B_3. In these experiments A_2 was an isocyanate end capped PTMO-2000, which was obtained by the reaction of PTMO-2000 with a two-fold excess of HMDI and B_3 was TRI. Chemical structures of these compounds are provided in Fig. 1. Isocyanate terminated oligomeric A_2 shown in Fig. 1, is the ideal structure. Actual A_2 has a distribution of molecular weights and some unreacted HMDI.

In order to monitor the growth in the molecular weight of the polymers formed, samples were withdrawn from the reactor at different amounts of A_2 addition and end capped with CHI prior to SEC analysis. Dendritic and hyperbranched structures are known to have different mass–hydrodynamic volume relationship compared to linear polymer standards that are used in SEC measurements. It should be noted that all SEC data reported in this manuscript are from MALLS detector. However, as we discuss in the manuscript, in our case, these highly branched structures also have linear segments between branch units, resembling structures between hyperbranched and long-chain branched polymers. Several hyperbranched poly(urethaneurea)s that were synthesized using the exact same methodology were also examined in hexafluoroisopropanol and both the molecular weight and the molecular weight distribution values were very close to the results obtained in THF [69]. Several studies that were reported on a variety of hyperbranched structures and their SEC characterization also demonstrated that SEC-viscometry can be useful [14,70]. Van Bentham and co-workers analyzed the size exclusion chromatography fractions of bis(2-hydroxypropyl)amide based hyperbranched polyesteramides by MALD/I-TOF MS, and confirmed that the masses measured were identical to those measured by SEC equipped with a viscometry detection. Recent review by Mourey also provides several examples on the agreement in the molecular weight measurements of hyperbranched polymers by SEC and other direct methods [70].

SEC chromatographs provided in Fig. 2 show the change in the molecular weight of the polymer formed as a function of oligomeric A_2 addition into B_3, where the concentration of the polymerization medium was constant at 25% solids by weight. Interestingly, gel point in this system was also observed at 89.0% A_2 addition, which is very similar to that of HMDI+TRI system described above, where experimental gel point was at 88.6% A_2 addition. Therefore, in SEC curves provided in Fig. 2, the highest level of A_2 incorporation was 84%. $\langle M_n \rangle$ and $\langle M_w \rangle$ values obtained from light scattering detector are tabulated in Table 2. SEC curves clearly show the increase in the molecular weight of the polymer formed as a function of the amount of A_2 addition. SEC chromatograms shown in Fig. 2, have two major peaks. The small peak centered at the elution volume of 24.5 min, which is due to B_3, becomes smaller as more A_2 is added. This is expected since B_3 concentration in the reaction mixture is reduced as it reacts with A_2. The large peak, which is due to the polymer formed, moves to lower elution volumes (minutes) as more A_2 reacts with B_3 and molecular weight of the polymer increases. SEC peaks are

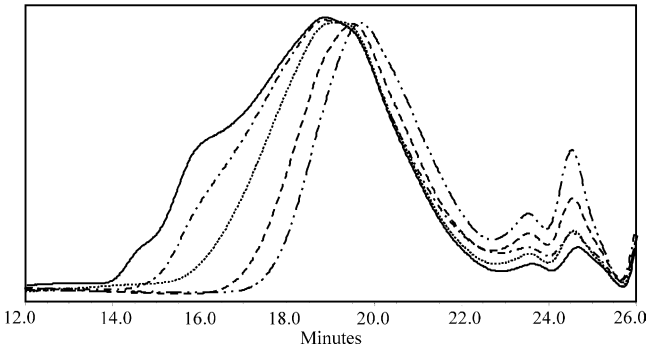

Fig. 2. Monitoring the molecular weight development in oligomeric A_2+B_3 polymerization as a function of mole percent of A_2 addition in the reaction between isocyanate terminated PTMO-2k+TRI; in THF/IPA (25/75 wt/wt); concentration of the reaction medium 25% solids by weight. (– - - –) 50%, (– – –) 60%, (- - -) 71%, (– - - - –) 76% and (—) 84% A_2 addition.

very symmetrical until very high levels of A_2 addition. This is a good indication which shows that slow addition of A_2 into B_3 results in homogeneous polymer growth. At 76% A_2 addition SEC curve shows a shoulder at lower elution volumes, indicating the formation of small amount of very high molecular weight polymer. At 84% A_2 addition two well defined shoulders can be seen on the SEC curve between 14 and 16 min elution volume. This is very typical for hyperbranched systems, where formation of very high molecular weight polymers are observed as the stoichiometric ratio of $[A_2]/[B_3]$ approaches to the gel point [1–6], which is at 75.0% A_2 addition during this reaction, as discussed before. When average M_n and M_w and molecular weight distribution or polydispersity index ($PI = M_w/M_n$) values for the polymers are examined (Table 2), a slow growth in M_n and M_w, typical of step-growth polymerization reactions are observed. Initially PI values of the oligomers/polymers formed are also around 1.5, also typical for condensation reactions. However, as more A_2 is added into the system and reacted with B_3, PI values of the polymer formed start increasing rapidly to 2.20, 4.06 and 5.88 at 71, 76 and 84% A_2 addition, respectively. This is a clear indication of the formation of highly branched polymers, which typically show fairly high PI values [6,52].

Table 3 summarizes the SEC results on average molecular weights and molecular weight distributions of the polymers formed as a function of the amount of oligomeric A_2 addition during the reaction of isocyanate terminated PTMO (A_2) and TRI (B_3), where the concentration of reaction medium was 10% solids by weight. As A_2 is added and reacted with B_3, a gradual increase in $\langle M_n \rangle$, $\langle M_w \rangle$ and PI is observed, similar to that of 25% solid system discussed above. After 95% A_2 addition the increase in $\langle M_w \rangle$ and PI become more drastic due to the formation of highly branched polymers. Gel point in these experiments is observed at 112% of the A_2 addition (i.e. $[A_2]/[B_3] = 1.12$). This is also in very good agreement with the low molecular weight A_2 (HMDI) + B_3 (TRI) system, where gel point was observed at 107.5% A_2 addition (i.e. $[A_2]/[B_3] = 1.075$).

Fig. 3 provides a direct comparison of the change in $\langle M_w \rangle$ as a function of oligomeric A_2 addition for polymerization reactions conducted at concentrations of 10 and 25% solids by weight. It is important to note that in both reactions the increase in $\langle M_w \rangle$ follows a very similar profile. The only difference is in the amount of A_2 needed to achieve similar $\langle M_w \rangle$ values for reactions carried out at different solution concentrations, due to dilution effects. In the reaction carried out at 25% solids, $\langle M_w \rangle$ values of the polymers formed are fairly low, less than 50,000 g/mol, until about 65% A_2 addition. Then as more A_2 is added a sharp upturn is observed and $\langle M_w \rangle$ reaches to 255,000 g/mol at 84% A_2 addition. A very similar behavior is observed in reactions conducted at 10% solids. As we have discussed in detail above, since the extent of cyclization is much higher at 10% solution than that of 25%, SEC results show formation of fairly low molecular weight polymers until about 85% A_2

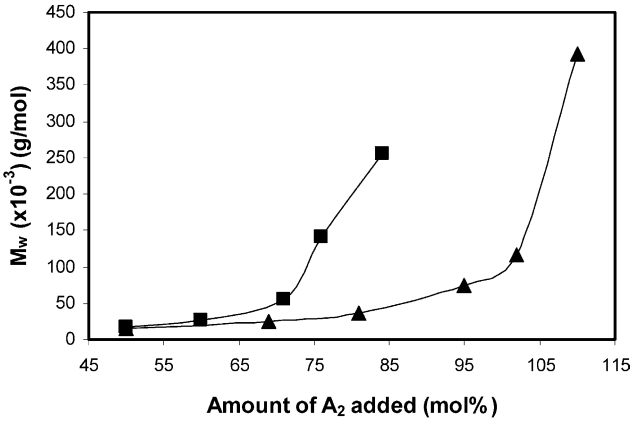

Fig. 3. Comparison of the change in $\langle M_w \rangle$ as a function of oligomeric A_2 addition for polymerization reactions conducted at concentrations of 10% (▲) and 25% (■) solids by weight.

addition, where $\langle M_w \rangle$ reaches to about 50,000 g/mol. At 95 and 102% A_2 additions $\langle M_w \rangle$ reaches to 75,000 and 116,000 g/mol, respectively. Then there is a very sharp increase in $\langle M_w \rangle$, reaching to 392,000 g/mol at 110% A_2 addition.

Fig. 4 provides a comparison of the change in PI for oligomeric $A_2 + B_3$ polymerization reactions conducted at concentrations of 10 and 25% solids by weight. In early stages of polymerization reactions, due to the stoichiometry of the mixture, where B_3 is in large excess, mainly B_3 terminated oligomers and polymers with low degrees of branching are produced. As a result in both 10 and 25% reactions PIs are below 2.0, typical for step-growth polymers. However, as the amount of A_2 incorporation increases a dramatic increase in PI values, which goes to about 6.0 are observed. This is a clear indication of the formation of highly branched polymers.

3.3. Monte-Carlo simulations

Monte-Carlo simulations were carried out with and without cyclization taken into account. On the other hand, the solvent effect was not taken into account during

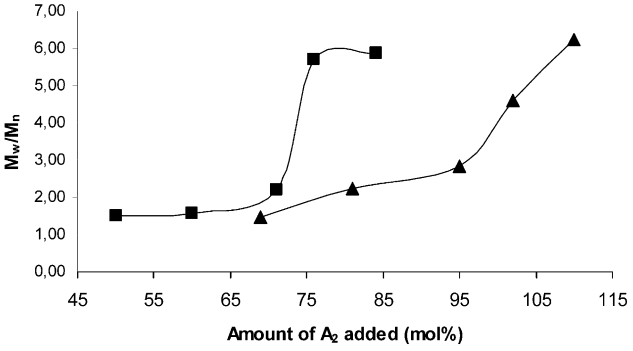

Fig. 4. Comparison of the change in polydispersity ($\langle M_w \rangle / \langle M_n \rangle$) as a function of oligomeric A_2 addition for polymerization reactions conducted at concentrations of (▲) 10% and (■) 25% solids by weight.

simulation studies. To mimic various levels of cyclization in the polymers formed, the simulations were carried out at different cyclization ratios, such as; $\gamma=0$ (no cyclization), $\gamma=0.01$ and $\gamma=0.1$ (low cyclization) and $\gamma=1$ (very high cyclization). Molecular weights of A_2 and B_3 are taken as 2500 and 440 g/mol, to mimic the experimental system based on isocyanate capped PTMO-2000 and TRI. The results obtained by simulation system containing 1000 (B_3) molecules were independent of the system size and therefore would be expected to yield polymer molecular weights in the same range as those obtained in the experiments. As it is clearly demonstrated in the following discussions, this assumption proved to be fairly reasonable. Similar to the experiments, during simulations oligomeric A_2 is added into B_3 slowly up to a stoichiometric ratio of $[A_2]:[B_3]=1.15$ or 115% A_2.

Fig. 5(a) and (b) shows the Monte-Carlo simulation results on the development of number $\langle M_n\rangle$ and weight average $\langle M_w\rangle$ molecular weights as a function of A_2 addition, for a 1000×1000 ($A_2\times B_3$) system. As depicted in Fig. 5(a), regardless of the cyclization ratio, a slow increase in $\langle M_n\rangle$ values were observed until a fairly large amount of A_2 (about 75%) is added into the system. This is followed by a sharp increase for polymers in which the cyclization is not taken into account, where $\langle M_n\rangle$ value 'theoretically' is expected to reach infinity, as predicted by Flory's theory [37,61]. As expected, the growth in the number average molecular weight $\langle M_n\rangle$ is severely limited for polymers that show moderate to high level of cyclization. As depicted in Fig. 5(a), even at the fairly low cyclization ratio of $\gamma=0.01$, at 100% A_2 addition, a very dramatic reduction in $\langle M_n\rangle$ is observed, where it only reaches to about 60,000 g/mol. At a cyclization ratio of 0.1, $\langle M_n\rangle$ is further reduced and reaches to only about 20,000 g/mol at 100% A_2 addition. Simulations performed assuming the highest cyclization ratio of $\gamma=1$ clearly show the formation of very low molecular weight products, which is expected. As clearly demonstrated in Fig. 5(b), cyclization has less of an effect on the development of $\langle M_w\rangle$. Even at a cyclization ratio of $\gamma=0.1$, $\langle M_w\rangle$ reaches to very high values. Only at the highest cyclization ratio of $\gamma=1$, similar to $\langle M_n\rangle$, there is a dramatic reduction in $\langle M_w\rangle$. Simulations clearly indicate that cyclization delays the onset of gel formation well beyond the theoretical A_2 conversion of 75.0%. In order to make a direct comparison, Fig. 6(a) and (b) gives the experimental results on M_n and M_w from Tables 2 and 3, together with the results of Monte-Carlo simulations. It is interesting to note that experimental M_n and M_w values obtained for polymerizations at 25% solids (Table 2) agree fairly well with simulations, where cyclization ratio is low ($\gamma=0$–0.01). Even more interestingly, experimental M_n and M_w values obtained for polymerizations at 10% solids (Table 3) agree very well with simulations where degree of cyclization is higher ($\gamma=0.1$).

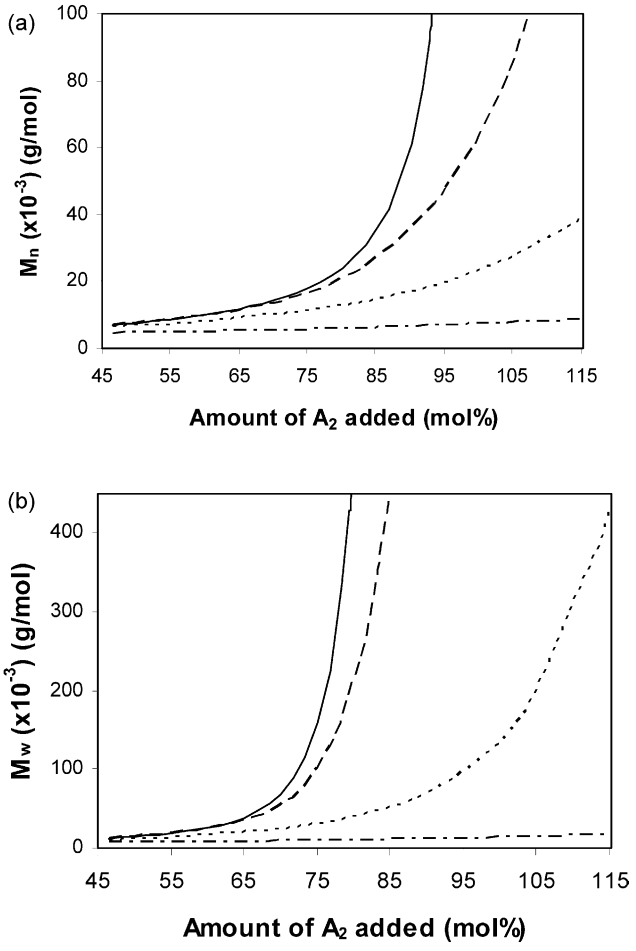

Fig. 5. Results of Monte-Carlo simulations on the development of average polymer molecular weight as a function of A_2 addition and cyclization ratio (γ) for a 1000×1000 ($A_2\times B_3$) system. (a) Number average molecular weight $\langle M_n\rangle$ and (b) weight average molecular weight $\langle M_w\rangle$. (—) $\gamma=0$, (– – –) $\gamma=0.01$, (- - -) $\gamma=0.1$, and (– – – – –) $\gamma=1$.

Fig. 7(a) and (b) shows simulation results on the polydispersity index (PI) and the degree of branching (DB) as a function of A_2 addition. As depicted in Fig. 7(a), PI shows a gradual increase as A_2 is added into the system and reacted with B_3. As expected, after about 60% A_2 addition there is a dramatic increase in PI for all systems, except for the case of very high cyclization, or when $\gamma=1$. These results agree very well with the experimental observations, which are plotted on Fig. 4. Simulation results on the degree of branching (DB) as a function of cyclization parameter (γ) and amount of A_2 added are depicted in Fig. 7(b). It is important to note that at the beginning of the simulations there is only B_3 in the system, so DB = 1.0. As A_2 is added into the system and reacts with B_3, DB starts going down slowly and levels off around 0.5–0.6 after about 80% A_2 addition for simulations where cyclization parameter is low ($\gamma=0$–0.1). Interestingly, for the system with highest cyclization parameter ($\gamma=1$), the behavior is quite different. Monte-Carlo simulations indicate that in this system with very high cyclization probability, even at low A_2 additions, DB starts around 0.75 and gradually moves to

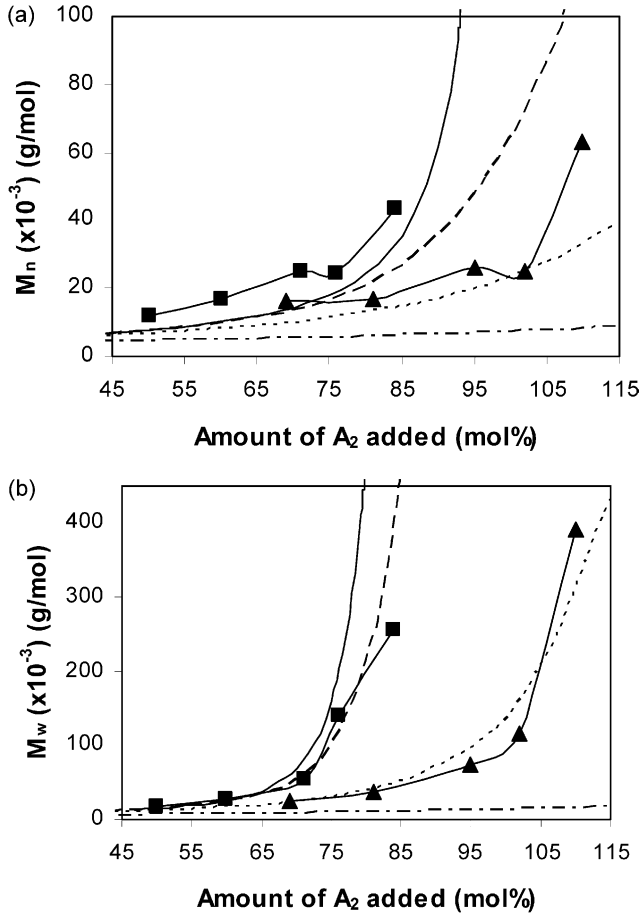

Fig. 6. Comparison of experimental and simulation results on the development of average polymer molecular weight as a function of A_2 addition and cyclization ratio (γ) for a 1000×1000 (A_2×B_3) system. (a) Number average molecular weight $\langle M_n \rangle$ and (b) weight average molecular weight $\langle M_w \rangle$. Experimental data: (■) from Table 2, and (▲) from Table 3. Simulation data: (—) $\gamma=0$, (– – –) $\gamma=0.01$, (- - -) $\gamma=0.1$, and (– - – - –) $\gamma=1$.

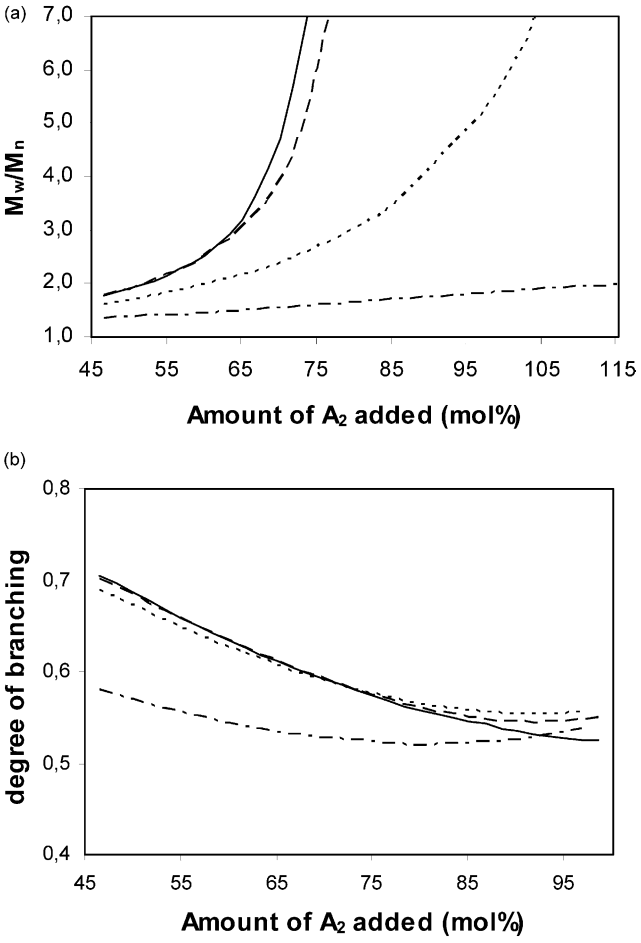

Fig. 7. Kinetic Monte-Carlo simulations on the polydispersity index (PI) Fig. 6(a) and the degree of branching (DB) Fig. 6(b) as a function of A_2 addition. (—) $\gamma=0$, (– – –) $\gamma=0.01$, (- - -) $\gamma=0.1$, and (– - – - –) $\gamma=1$.

about 0.5–0.6 similar to the other systems. Frey has pointed out that [71] DB statistically approaches to 0.5 in case of polymerization of AB_2 monomers, calculated using DB = (D + T)/(D + L + T) [72]. Although our system is designated as A_2+B_3, since we add A_2 slowly onto B_3 we actually form AB_2 in situ during simulations (and reactions). Our simulations resulted in a DB value of 0.53 at complete A_2 addition without cyclization. This is in excellent agreement with simulations of Frey [71] and also with the DB values observed experimentally in A_2+B_3 systems [19]. With the inclusion of cyclization, DB goes up slightly from this value of 0.53, as clearly shown in Fig. 7(b).

Another important characteristic of such highly branched polymers, the number of cyclization events per molecule, as a function of A_2 conversion is shown in Fig. 8. For small cyclization ratios ($\gamma=0.01$ and $\gamma=0.1$) and low conversions, the number of cyclic species per molecule are negligible until about 80% A_2 addition. As the amount of A_2 exceeds 80% and high molecular weight polymers are obtained, cyclization increases and reaches to about 2 per molecule. Interestingly, simulation results given in Fig. 8 on the amount of cyclization per molecule, for high cyclization ratio (e.g. $\gamma=1$) and high conversions seems to be

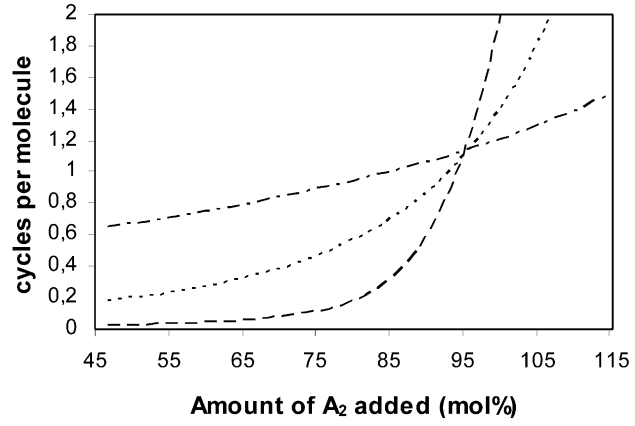

Fig. 8. Number of cyclization events per molecule, as predicted by the kinetic Monte-Carlo simulations as a function of A_2 addition, at different levels of cyclization. (– – –) $\gamma=0.01$, (- - -) $\gamma=0.1$, and (– - – - –) $\gamma=1$.

somewhat contradictory to expectations, since they are much smaller. However, since the molecular weight of the polymer formed is strongly suppressed due to extensive cyclization, in these simulations polymers formed have very low molecular weights (Fig. 5(a) and (b)). In other words, in these cases only very small molecules which also have a smaller total number of cycles are formed.

4. Conclusions

Formation of highly branched, segmented polyurethaneureas based on oligomeric A_2+B_3 approach, where A_2 is slowly added onto B_3 were investigated by experimental studies and kinetic Monte-Carlo simulations. SEC results clearly demonstrated the formation of high molecular weight segmented copolymers with very high polydispersity values, typical of highly branched polymers. When polymerization reactions are conducted in dilute solutions no gelation was observed even at stoichiometric ratios of $[A_2]/[B_3]$ well beyond the theoretical gel point of 0.75. This is attributed to high degree of cyclization in dilute solutions. Results obtained from kinetic Monte-Carlo simulations were in very good agreement with the experimental observations.

Acknowledgements

This material is based upon work supported by, or in part by, the US Army Research Laboratory and the US Army Research Office under grant number DAAD19-02-1-0275 Macromolecular Architecture for Performance (MAP) MURI and by the US Air Force Office of Scientific Research under FA9550-04-1-0183.

References

[1] Kim YH. J Polym Sci, Part A: Polym Chem 1998;36:1685–98.
[2] Voit B. J Polym Sci, Part A: Polym Chem 1998;38:2505–25.
[3] Jikei M, Kakimoto M. Prog Polym Sci 2001;26:1233–85.
[4] Hult AH, Johansson H, Malmström E. Adv Polym Sci 1999;143:1–34.
[5] Yates CR, Hayes W. Eur Polym J 2004;40:1257–81.
[6] Gao C, Yan D. Prog Polym Sci 2004;29:183–275.
[7] Kricheldorf HR, Zang Q-Z, Schwartz G. Polymer 1982;23:1821–9.
[8] Hawker CJ, Lee R, Frechet JMJ. J Am Chem Soc 1991;113:239–48.
[9] Trollsas M, Atthoff B, Claesson H, Hedrick JL. Macromolecules 1998;31:3439–45.
[10] Trolsas M, Hedrick JL. Macromolecules 1998;31:4390–5.
[11] Kim YH. J Am Chem Soc 1992;114:4947–8.
[12] Hao J, Jikei M, Kakimoto M. Macromolecules 2003;36:3519–28.
[13] Monticelli O, Mariani A, Voit B, Komber H, Mendichi R, Pitto V, et al. High Perform Polym 2001;13:S45–S59.
[14] van Benthem RATM, Meijerink N, Gelade E, de Koster CG, Muscat D, Froehling PE, et al. Macromolecules 2001;34:3559–66.
[15] Kim YH, Webster OW. J Am Chem Soc 1990;112:4592–3.
[16] Kim YH, Webster OW. Macromolecules 1992;25:5561–72.
[17] Martinez CA, Hay AS. J Polym Sci, Part A: Polym Chem 1997;35:1781–98.
[18] Lin Q, Long TE. J Polym Sci, Part A: Polym Chem 2000;38:3736–41.
[19] Czupik M, Fossum E. J Polym Sci, Part A: Polym Chem 2003;41:3871–81.
[20] Miller TM, Neenan TX, Kwock EW, Stein SM. J Am Chem Soc 1993;115:356–7.
[21] Hawker CJ, Chu F. Macromolecules 2001;33:4370–80.
[22] Srinivasan S, Twieg R, Hedrick JL, Hawker CJ. Macromolecules 1996;29:8543–5.
[23] Sunder A, Hanselmann R, Frey H, Mülhaupt R. Macromolecules 1999;32:4240–6.
[24] Spindler R, Frechet JMJ. Macromolecules 1993;26:4809–13.
[25] Kumar A, Ramakrishnan S. J Chem Soc Chem Commun 1993;1453–4.
[26] Kumar A, Ramakrishnan S. J Polym Sci, Part A: Polym Chem 1996;34:839–48.
[27] Bruchmann B, Schrepp W. e-Polymer 2003 [no. 014].
[28] Feast WJ, Rannard SP, Stoddart A. Macromolecules 2003;36:9704–6.
[29] Gao C, Yan D. Macromolecules 2003;36:613–20.
[30] Kumar A, Meijer EW. J Chem Soc Chem Commun 1998;1629–30.
[31] Bolton DH, Wooley KL. Macromolecules 1997;30:1890–6.
[32] Burchard W. Adv Polym Sci 1999;143:113–94.
[33] Dusek K, Somvarsky J, Smrekova M, Simonsick Jr WJ, Wilczek L. Polym Bull 1999;42:489–96.
[34] Hanselmann R, Hoelter D, Frey H. Macromolecules 1998;31:3790–801.
[35] Perez MA, Longo E, Taft CA. J Mol Struct (Theochem) 2000;507:97–110.
[36] Galina H, Lechowicz JB, Kaczmarski K. Macromol Theory Simul 2001;10:174–8.
[37] Flory PJ. J Am Chem Soc 1952;74:2718–23.
[38] Hepburn C. Polyurethane elastomers. Essex: Elsevier Science Publishers; 1992.
[39] Lelah MD, Cooper SL. Polyurethanes in medicine. Boca Raton: CRC Press; 1986.
[40] Oertel G. Polyurethanes handbook. Munich: Hanser Publishers; 1994.
[41] Woods G. The ICI polyurethanes book. New York: Wiley; 1990.
[42] Yilgor E, Yilgor I. Polymer 2001;42:7953–9.
[43] Saiani A, Daunch WA, Verbeke H, Leenslang JV, Higgins JS. Macromolecules 2001;34(26):9059–68.
[44] Garrett JT, Runt J, Lin JS. Macromolecules 2000;33(17):6353–9.
[45] Hong L, Cui Y, Wang X, Tang X. J Polym Sci, Part A: Polym Chem 2002;40:344–50.
[46] Davis N, Rannard S. Polym Mater Sci Eng 1997;77:63–4.
[47] Versteegen RM, Sijbesma RP, Meijer EW. Polym Prepr 1999;40(2):839–40.
[48] Taylor RT, Paupailboon U. Tetrahedron Lett 1998;39:8005–8.
[49] Bruchmann B, Koeniger R, Renz H. Macromol Symp 2002;187:271–9.
[50] Bruchmann B, Ehe U, Wingerter F, Stiefenhoefer K, Treuling U. DE 19904444, (BASF AG); 1999.
[51] Yilgor I, Unal S, Yilgor E, Long TE. US Patent Disclosure (Virginia Tech); 2003.
[52] Unal S, Yilgor I, Yilgor E, Sheth JP, Wilkes GL, Long TE. Macromolecules 2004;37:7081–3.
[53] Yilgor I, Mather B, Unal S, Yilgor E, Long TE. Polymer 2004;45:5829–36.
[54] Radke W, Litvinenko G, Mueller AHE. Macromolecules 1998;31:239–48.
[55] Somvarsky J, Dusek K. Polym Bull 1994;33:369–76.
[56] Lescanec RL, Muthukumar M. Macromolecules 1993;23:2280–8.
[57] Gong C, Miravet J, Frechet JMJ. J Polym Sci, Part A: Polym Chem 1999;37:3193–201.
[58] Kricheldorf HR, Schwartz G. Macromol Rapid Commun 2003;24:359–81.

[59] Vakhtangishvili L, Fritsch D, Kricheldorf HR. J Polym Sci, Part A: Polym Chem 2002;40:2967.
[60] Bortz AB, Kalos MH, Lebowitz JL. J Comp Phys 1975;17:10–15.
[61] Flory PJ. Chem Rev 1946;39:137–97.
[62] Kricheldorf HR. Macromolecules 2003;36:2302–8.
[63] Gooden JK, Gross ML, Mueller A, Stefanescu AD, Wooley KL. J Am Chem Soc 1998;120:10180–6.
[64] Martinez CA, Hay AS. J Polym Sci, Part A: Polym Chem 1997;35: 2015–33.
[65] Ziegler K. Ber Dtsch Chem Ges 1934;67A:139.
[66] Jacobsen H, Stockmayer WH. J Chem Phys 1950;18:1600.
[67] Jacobsen H, Beckmann CO, Stockmayer WH. J Chem Phys 1950;18: 1607.
[68] Semlyen JA. Large ring molecules. New York: Wiley; 1996 [chapter 1].
[69] Sheth JP, Unal S, Yilgor E, Yilgor I, Beyer FL, Long TE, et al. Polymer. Submitted for publication.
[70] Mourey TH. Int J Polym Anal Charact 2004;9:97–135.
[71] Holter D, Burgath A, Frey H. Acta Polym 1997;48:30–5.
[72] Hawker CJ, Lee R, Frechet JMJ. J Am Chem Soc 1991;113:4583–8.